

Catalytic ring-attachment isomerization and dealkylation of diethylbenzenes over halide clusters of group 5 and group 6 transition metals

Satoshi Kamiguchi,^a Kunihiko Kondo,^b Mitsuo Kodomari,^b and Teiji Chihara^{a,*}

^a Institute of Physical and Chemical Research (RIKEN), Wako, Saitama 351-0198, Japan

^b Department of Applied Chemistry, Shibaura Institute of Technology, Shibaura, Minato-ku, Tokyo 108-8548, Japan

Received 29 September 2003; revised 6 January 2004; accepted 6 January 2004

Abstract

A molybdenum halide cluster, $(\text{H}_3\text{O})_2[(\text{Mo}_6\text{Cl}_8)\text{Cl}_6] \cdot 6\text{H}_2\text{O}$, possessing an octahedral metal framework was used as a catalyst in a gas flow reactor under 1 atm of hydrogen. On reaction of *p*-diethylbenzene, dehydrogenation to ethylstyrene proceeded selectively at 300 °C. At 400 °C, mutual interconversion of *o*-, *m*-, and *p*-diethylbenzenes proceeded selectively. The ethyl group migrated by an intramolecular 1,2-shift mechanism without yielding disproportionation products. Niobium and tungsten chloride clusters with the same metal framework were also active catalysts for the isomerization of *p*-diethylbenzene. All the reactions resulted in appreciable yields of dealkylation products. The catalytic activity for isomerization can be ascribed to acid sites on the cluster surface, and the catalytic activity for dealkylation, to the metallic nature of the framework metal.

© 2004 Elsevier Inc. All rights reserved.

Keywords: Isomerization; Dealkylation; Dehydrogenation; Diethylbenzene; Halide cluster; Molybdenum halide; Tungsten chloride; Niobium chloride; Tantalum chloride

1. Introduction

We have previously reported on the catalytic activity of halide clusters in the isomerization of olefins [1], dehydrohalogenation of halogenated alkanes [2], dehydration of alcohols [3], and decomposition of phenyl acetate to phenol and ketene [4]. Although these reactions are common, and are catalyzed mostly by solid acids, halide cluster catalysts exhibit characteristic features in their selectivity and activity. We have carried out many reactions to broaden our knowledge on the application of these new catalysts and to shed light on their characterization from a reactivity point of view. Some of the attempted reactions were successful and, in this article, a unique intramolecular ring-attachment isomerization of *p*-diethylbenzene to *o*- and *m*-diethylbenzenes and related reactions are presented.

Much literature has appeared on the catalytic ring-attachment isomerization of *o*- and *m*-xylenes and the cat-

alytic intermolecular transalkylation (disproportionation) of toluene to produce *p*-xylene [5,6], which is used in its oxidation to form terephthalic acid, and the subsequent reaction with ethylene glycol to synthesize polyester resins. Mordenite and ZSM-5 are currently the best catalysts for those catalytic reactions [7–9]. Chemical modification with antimony [10], chemical vapor deposition of tetraethoxysilane [11], and chemical liquid deposition of tetraethoxysilane [12] were reported to increase the selectivity of ZSM-5. Trimethylbenzenes and bulkier polymethylbenzenes were allowed to react over medium- and large-pore zeolites. Zeolites NU-87 that have 12-membered ring pockets on the crystal surface disproportionated trimethylbenzenes largely within the micropores, while the isomerization reaction occurred mainly on the external surface [13]. Similarly, large-pore zeolite Beta disproportionated trimethylbenzenes [14], tetramethylbenzene, pentamethylbenzene, and hexamethylbenzene [15]. Over the mesoporous molecular sieve of MCM-41, the disproportionation of trimethylbenzenes is also reported [16]. On the large-pore aluminophosphate molecular sieve of substituted AlPO-5 materials, disproportionation competed with isomerization. The disproportiona-

* Corresponding author.

E-mail address: chihara@postman.riken.go.jp (T. Chihara).

tion of trimethylbenzenes and toluene occurred on stronger acid sites, while the isomerization of trimethylbenzenes and xylenes predominated on weaker acid sites [17]. On the other hand, very little has been reported on the reactions of ethylbenzene and diethylbenzenes, even though *p*-diethylbenzene is an industrial source of *p*-divinylbenzene.

Some strong molecular acids have been used as homogeneous catalysts in solution. The catalytic disproportionation of ethylbenzene in the presence of AlCl_3 yielded benzene, *m*- and *p*-diethylbenzenes, and 1,2,4-triethylbenzene [18]. In an AlCl_3 –HCl catalytic system, the disproportionation of *m*- and *p*-diethylbenzenes proceeded to yield ethylbenzene and 1,2,4-triethylbenzene [19]. A protic acid, CF_3COOH , also catalyzed the disproportionation of *m*-diethylbenzene to yield ethylbenzene and 1,2,4-triethylbenzene by an ethylcarbenium rearrangement [20]. All of these catalytic reactions were intermolecular transalkylations. On the other hand, apparent interconversions of *o*-, *m*-, and *p*-diethylbenzenes have been reported in the presence of an AlCl_3 catalyst, and the isomerization was attributed solely to a sequence involving an intramolecular 1,2-shift mechanism [21]. This conclusion is doubtful, because disproportionation products account for as much as 40% of the products [22]. The isomerization of *p*-substituted toluenes catalyzed by AlCl_3 has been reported, and only xylenes were isomerized exclusively via an intramolecular 1,2-shift mechanism. The isomerization of *t*-butyltoluene proceeded by an intermolecular alkyl transfer mechanism, and the isomerization of ethyltoluenes and isopropyltoluenes proceeded by both of the above mechanisms [23,24]. On the basis of this result, the isomerization of diethylbenzenes should follow both the above mechanisms in the presence of AlCl_3 . In summary, the ring-attached ethyl group undergoes mainly intermolecular migration by the homogeneous acid catalysts such as AlCl_3 , AlCl_3 –HCl, and CF_3COOH .

Similarly, diethylbenzenes disproportionated over solid catalysts. When Y-zeolite mixed with SiO_2 – Al_2O_3 was employed as a catalyst in a neat liquid of *o*-, *m*-, or *p*-diethylbenzene at 170 °C, disproportionation occurred, affording ethylbenzene and 1,2,4-triethylbenzene. Although small yields of *o*-, *m*-, and *p*-diethylbenzenes were formed, they were the secondary intermolecular transalkylation products from ethylbenzene and 1,2,4-triethylbenzene [22]. Disproportionation of ethylbenzene to afford benzene and *m*- and *p*-diethylbenzenes was reported over a ZSM-5 catalyst without yielding *o*-diethylbenzene [25]. In this case, *o*-diethylbenzene was too large to locate in the ZSM-5 cavities [26]. Similarly, the exclusive formation of *p*-diethylbenzene over ZSM-5 has been reported in the reaction of ethylbenzene with ethylene on a commercial scale [7] or with ethanol in the laboratory [27]. In the latter case, the *p*-diethylbenzene produced subsequently isomerizes to form the *meta*-isomer. Generally, in large-pore zeolites, such as Y-zeolites and mordenite, side chains disproportionate by way of bimolecular transalkylation. Conversely, in medium-pore zeolites, such as ZSM-5, disproportionation proceeds

by way of successive dealkylation and realkylation [28]. Thus, ring-attached ethyl groups do not migrate around the aromatic ring by an intramolecular 1,2-shift mechanism over conventional heterogeneous solid acid catalysts.

2. Experimental

2.1. Materials and characterization

The cluster complexes $[(\text{Nb}_6\text{Cl}_{12})\text{Cl}_2(\text{H}_2\text{O})_4] \cdot 4\text{H}_2\text{O}$ [29], $(\text{H}_3\text{O})_2[(\text{Mo}_6\text{Cl}_8)\text{Cl}_6] \cdot 6\text{H}_2\text{O}$ (**1**) [30], $[(\text{Mo}_6\text{Br}_8)(\text{OH})_4(\text{H}_2\text{O})_2]$ [31], $[(\text{Ta}_6\text{Cl}_{12})\text{Cl}_2(\text{H}_2\text{O})_4] \cdot 4\text{H}_2\text{O}$ [29], and $(\text{H}_3\text{O})_2[(\text{W}_6\text{Cl}_8)\text{Cl}_6] \cdot 6\text{H}_2\text{O}$ [32] were prepared according to published procedures, followed by repeated recrystallization to yield well-formed single crystals. Commercial Re_3Cl_9 (Furuya Metal) was used without further purification. The crystals of the above complexes were crushed until they passed through a 150-mesh screen, but not a 200-mesh screen. Solid-state clusters of $[\text{Mo}_6\text{Cl}_8^i\text{Cl}_2^a\text{Cl}_{4/2}^{a-a}]$ (**2**), were obtained by heating **1** at a rate of 100 °C/h to 200 °C, followed by a dwell at 200 °C for 6 h under vacuum [30]. Organic substrates employed were commercial products, and were used as received.

The Raman spectra of the cluster samples in glass reaction tubes employed were recorded in situ on a Kaiser Optical Systems HoloLab 5000 Spectrometer using a Nd-YAG laser operating at $\lambda = 532$ nm, with a 7.6-mm focusing lens. The data counts were accumulated 30 times over 1-s intervals. Then, the cluster samples were transferred to an airtight sample holder in a globe box, and powder X-ray diffraction (XRD) was performed on 20-mg samples using a MacScience MXP21TA-PO X-ray diffractometer employing $\text{Cu-K}\alpha$ radiation and a scan rate of 2°/min.

The trapped reaction products were analyzed using a Hewlett–Packard 5890 Series II gas chromatograph coupled with a Jeol Automass System II analyzer, with a 15-m \times 0.25-mm \times 0.25- μm DB-1 capillary column and helium carrier gas (GC/MS), and a GL Sciences 353B gas chromatograph (GLC) with a flame ionization detector, a 30-m \times 0.25-mm \times 0.25- μm DB-1 capillary column, and helium carrier gas. In the GLC analysis, all the products were identified by comparison with authentic commercial samples. The catalytic activities were evaluated using an on-line Shimadzu 14B gas chromatograph. This was fitted with a flame ionization detector, a 9.5-m \times 3-mm 10% Bentone 34 on Neopack 1A-packed column to study the reaction of diethylbenzenes, a 2-m \times 3-mm 5% Bentone 34 and 5% dinonyl phthalate (DNP) on Shimalite-packed column for the reactions of *p*-xylene, a 2-m \times 3-mm 5% Bentone 34 and 5% DNP on Shimalite-packed column connected to a 3-m \times 3-mm 5% Bentone 34 and 5% di-*iso*-decyl phthalate on Uniport HP-packed column to study the reactions of *p*-ethyltoluene. The GLC used nitrogen as the carrier gas. The gaseous products were identified by using the on-line GLC employing a 3-m \times 3-mm Unipaks-packed column.

2.2. Apparatus and procedures

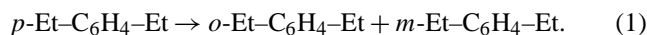
Gas flow reactions were carried out in a conventional apparatus [1]. The gas flow rate (300 mL/h) was controlled by an orifice-type flow regulator at ambient pressure, and the gas was introduced into a temperature-controlled stainless-steel tube with a glass lining (length = 3 m, i.d. = 2 mm), which was used as a preheater to heat the carrier gas to the same temperature as the reactor. The general procedure consisted of packing a known mass of the cluster complex (200 mg) in an electrically heated vertical tubular borosilicate glass reactor (i.d. = 3 mm) with the aid of quartz glass wool. Catalyst pretreatment was performed in situ immediately before the reaction under a stream of gas at the operating temperature for 1 h. Then, the liquid reactant was introduced at a controlled rate (0.40 mmol/h) via a motor-driven glass syringe pump through a T-joint attached before the reactor vessel. The products were introduced into a temperature-controlled gas sampler (1 mL) connected to a six-way valve, and were analyzed using the on-line GLC. The reactor effluent was frozen in a dry-ice trap for subsequent analysis, which was performed using the capillary column GLC. Preliminary experiments showed that the gaseous products were composed of methane, ethane, and ethylene.

In a typical experiment, a weighed cluster sample of $(\text{H}_3\text{O})_2[(\text{Mo}_6\text{Cl}_8)\text{Cl}_6] \cdot 6\text{H}_2\text{O}$ (**1**) (200 mg) was placed in the glass reaction tube surrounded by a close-fitting copper tube, which was placed in the center of an electric furnace. The catalyst sample was heated from room temperature to 400 °C, and maintained at that temperature for 1 h in a stream of hydrogen (300 mL/h) before a kinetic run. After a period of 10 min, the temperature reached the set point. The reaction was initiated by feeding neat *p*-diethylbenzene (62 $\mu\text{L/h}$, 0.40 mmol/h) into the stream of hydrogen using a microfeeder. Analysis of the trapped products showed that the material balance on recovery, based on aromatic compounds, was 95% (3–5 h). Formation of methane, ethane, and ethylene was detected by the gas analyses. The reaction was monitored every 20 min by sampling the reaction gas (1 mL) using the six-way valve, which was kept at 135 °C, followed by analysis using the on-line GLC. In this article, the conversion and selectivity are discussed on the basis of the data from the on-line GLC analysis.

3. Results and discussion

3.1. Reactions

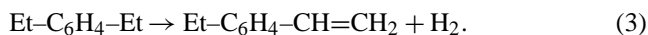
Ring-attachment isomerization



Dealkylation of the side chain (dealkylation of the ring attached alkyl)



Dehydrogenation



Intermolecular transalkylation (disproportionation)



Dealkylation in the side chain



3.2. Activation of $(\text{H}_3\text{O})_2[(\text{Mo}_6\text{Cl}_8)\text{Cl}_6] \cdot 6\text{H}_2\text{O}$ (**1**)

To assign their catalytic activity, the halide cluster complexes were employed in the form of crushed granules, which compromised their catalytic efficiency. The specific surface area of the crushed and screened crystals of $(\text{H}_3\text{O})_2[(\text{Mo}_6\text{Cl}_8)\text{Cl}_6] \cdot 6\text{H}_2\text{O}$ (**1**) was 3.95 m²/g.

When crystals of **1** in a glass reaction tube were treated in a stream of hydrogen at 400 °C for 1 h, and then allowed to react with *p*-diethylbenzene, a catalytic reaction proceeded. The reaction profile is shown in Fig. 1. The catalytic activity fluctuated with time, but leveled off after 3 h. The main reaction was the ring-attachment isomerization of Eq. (1), which yielded *m*-diethylbenzene in 74.0% selectivity, with a smaller yield of *o*-diethylbenzene in 7.7% selectivity. Dealkylation of the side chains (Eq. (2)) to yield ethylbenzene and benzene and dehydrogenation (Eq. (3)) to yield *p*-ethylstyrene proceeded to a small extent. However, no intermolecular transalkylation (Eq. (4)) to yield ethylbenzene and triethylbenzene was observed.

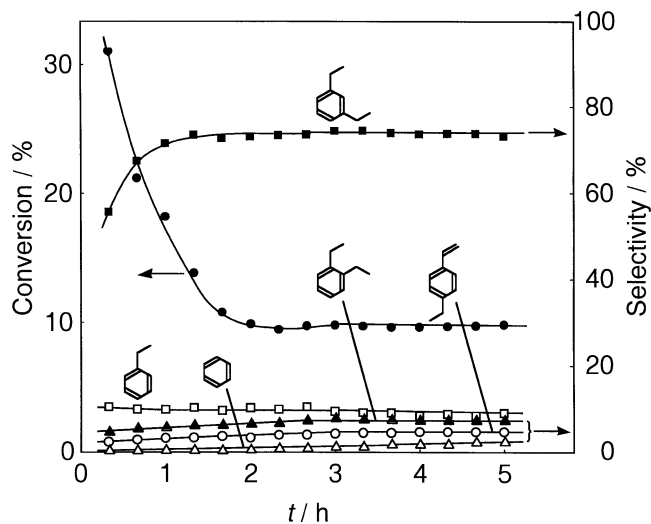


Fig. 1. Typical reaction profile of *p*-diethylbenzene over $(\text{H}_3\text{O})_2[(\text{Mo}_6\text{Cl}_8)\text{Cl}_6] \cdot 6\text{H}_2\text{O}$ (**1**). After treatment of **1** (200 mg) in a stream of H_2 (300 mL/h) at 400 °C for 1 h, the reaction was initiated by introducing *p*-diethylbenzene (0.40 mmol/h, 0.62 $\mu\text{L/h}$) to the H_2 stream at the same temperature. Percentage conversion = (reacted material)/(reacted material + recovered material) \times 100. Percentage selectivity = (product/(total amount of products)) \times 100. Methane, ethane, and ethylene originating from the side chain are not taken into account, but one carbon atom of those molecules originated from the aromatic ring equated to one-sixth of the reacted material.

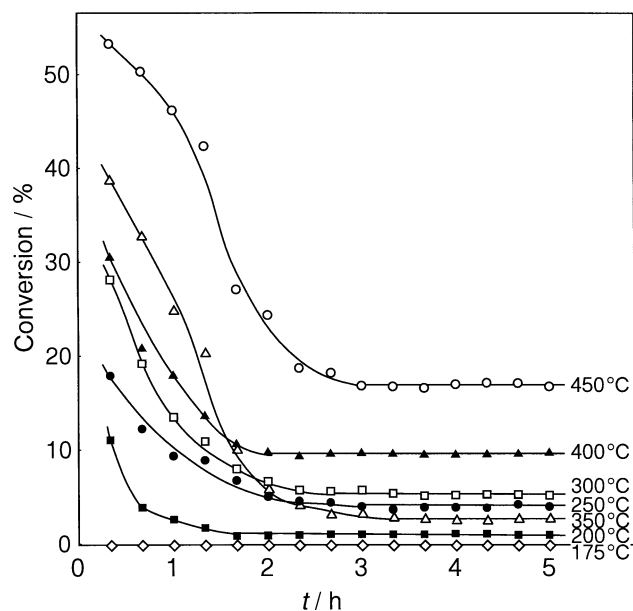


Fig. 2. Reaction profile of *p*-diethylbenzene catalyzed by $(\text{H}_3\text{O})_2[(\text{Mo}_6\text{Cl}_8)\text{Cl}_6] \cdot 6\text{H}_2\text{O}$ (**1**) at different temperatures. The other reaction conditions are the same as those described in the caption to Fig. 1.

The effect of temperature on the reactions over **1** was examined, and the reaction profiles at various temperatures are shown in Fig. 2. No catalytic activity was observed below 175 °C, and reactions above 200 °C showed substantial catalytic activity. Cluster **1** is a catalytically inactive and coordinatively saturated stable complex without multiple metal–metal bonds and, hence, was changed to an active species by the thermal treatment. The activity varied with time, but reached steady states after 3 h. The steady-state activities were not proportional to the temperature. The activity and composition of the products at various temperatures are plotted in Fig. 3. At 300 °C, the main reaction occurring was dehydrogenation (Eq. (3)) to yield *p*-ethylstyrene in 90% selectivity; however, at 400–475 °C this changed to ring-attachment isomerization (Eq. (1)) to afford *m*-diethylbenzene. At higher temperatures, near 500 °C, dealkylation of the side chain (Eq. (2)) proceeded more to completion with increasing temperature, yielding ethylbenzene and benzene. Thus, selectivity depended strongly on temperature. Different selectivity has been reported with faujasite [33]. When faujasite was used at 500–568 °C under cracking conditions, *p*-diethylbenzene yielded a large range of products by radical and ionic mechanisms. In this case, dehydrogenation yielded *p*-ethylstyrene as the main reaction, with dealkylation yielding ethylbenzene and *p*-ethyltoluene to a small extent, with traces of isomerization products.

3.3. Activity of halide clusters

Table 1 lists the catalytic activities of various halide clusters and related compounds treated in the same way at 400 °C. Molybdenum metal showed no catalytic activity un-

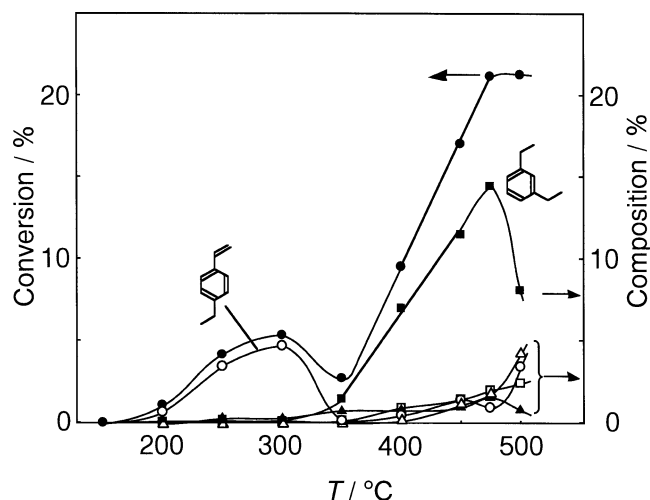


Fig. 3. Effect of temperature on the reactivity and product distribution of *p*-diethylbenzene over $(\text{H}_3\text{O})_2[(\text{Mo}_6\text{Cl}_8)\text{Cl}_6] \cdot 6\text{H}_2\text{O}$ (**1**) 4 h after the reaction was initiated. No hydrogenolysis of the aromatic ring was observed 4 h after the reaction started. Methane, ethane, and ethylene originating from the side chain are ignored in the calculation of composition. The other reaction conditions are the same as those described in the caption to Fig. 1. Conversion (●), *m*-diethylbenzene (■), *o*-diethylbenzene (▲), *p*-ethylstyrene (○), benzene (△), ethylbenzene (□). Products constituting less than 1% of the products have been omitted.

der the same reaction conditions, as did the example with no catalyst (entries 13 and 14 in Table 1). Molybdenum pentachloride cannot be applied as a catalyst under the same reaction conditions, as it boils at 268 °C. From these results, we inferred that the halide cluster **1** would serve as a catalyst precursor by taking advantage of its low vapor pressure and high melting point. The conversion was proportional to the mass of **1** used, and the reaction rate was of zero order with respect to the mass of *p*-diethylbenzene added, insofar as the conversion was not high and the added mass of *p*-diethylbenzene was not small. The conversion was proportional to the volume of carrier gas (entries 2–4), where *p*-diethylbenzene was in saturated adsorption. The effect of pretreatment temperature was examined. The catalytic activity of **1** treated at 300 °C throughout was about half that of **1** treated at 400 °C (entries 2 and 6). The former temperature afforded the dehydrogenation product, *p*-ethylstyrene, selectively. When a 400 °C pretreatment of **1** was applied to the reaction at 300 °C, the selectivity was the same as that of **1** treated at 300 °C throughout (entries 5 and 6). Hence, selectivity does not depend on pretreatment temperature, but on reaction temperature.

When the reaction was performed in a helium stream in the same manner, catalytic activity decreased noticeably, and its selectivity changed (entry 7). Dehydrogenation yielding *p*-ethylstyrene replaced isomerization as the main reaction, indicating that hydrogen plays an important role in the reaction. In a nitrogen stream, no reaction was observed. Diffusion of the reactant onto the cluster surface may be hindered in a viscous gas [34]. Alternatively, nitrogen could be adsorbed onto the Mo metal sites of activated **1**.

Table 1
Isomerization, dehydrogenation, and dealkylation of *p*-diethylbenzene over halide clusters^a

| Entry | Cluster | Carrier gas | Reaction temp. (°C) | Conversion (%) | Selectivity (%) | | | | | | | |
|-------|---|-----------------------------|---------------------------|-------------------|--------------------------|--------------------------|------------------------|--------------------------|--------------|---------|--------------|------------------------|
| | | | | | Isomerization | | Dehydrogenation | | Dealkylation | | | |
| | | | | | <i>o</i> -Diethylbenzene | <i>m</i> -Diethylbenzene | <i>p</i> -Ethylstyrene | <i>p</i> -Divinylbenzene | Benzene | Toluene | Ethylbenzene | <i>p</i> -Ethyltoluene |
| 1 | [(Nb ₆ Cl ₁₂)Cl ₂ (H ₂ O) ₄] · 4H ₂ O | H ₂ | 400 | 4.9 | 10.2 | 51.7 | 21.2 | 0.0 | 1.6 | 0.8 | 9.4 | 5.1 |
| 2 | (H ₃ O) ₂ [(Mo ₆ Cl ₈)Cl ₆] · 6H ₂ O (1) | H ₂ | 400 | 9.5 | 7.7 | 74.0 | 4.9 | 0.0 | 2.7 | 0.5 | 9.4 | 0.8 |
| 3 | (H ₃ O) ₂ [(Mo ₆ Cl ₈)Cl ₆] · 6H ₂ O (1) | H ₂ ^b | 400 | 14.6 | 4.5 | 77.3 | 3.9 | 0.0 | 4.0 | 0.6 | 9.2 | 0.5 |
| 4 | (H ₃ O) ₂ [(Mo ₆ Cl ₈)Cl ₆] · 6H ₂ O (1) | H ₂ ^c | 400 | 28.1 | 5.3 | 70.5 | 2.4 | 0.0 | 7.1 | 1.0 | 13.2 | 0.6 |
| 5 | (H ₃ O) ₂ [(Mo ₆ Cl ₈)Cl ₆] · 6H ₂ O (1) | H ₂ | 300 ^d | 3.4 | 2.1 | 4.0 | 90.3 | 0.0 | 0.2 | 0.4 | 1.7 | 1.3 |
| 6 | (H ₃ O) ₂ [(Mo ₆ Cl ₈)Cl ₆] · 6H ₂ O (1) | H ₂ | 300 ^e | 5.4 | 4.1 | 4.1 | 87.0 | 2.7 | 0.2 | 0.2 | 0.7 | 1.0 |
| 7 | (H ₃ O) ₂ [(Mo ₆ Cl ₈)Cl ₆] · 6H ₂ O (1) | He | 400 | 1.7 | 7.7 | 10.6 | 58.8 | 0.0 | 7.1 | 0.7 | 7.5 | 7.6 |
| 8 | (H ₃ O) ₂ [(Mo ₆ Cl ₈)Cl ₆] · 6H ₂ O (1) | N ₂ | 400 | 0.0 | – | – | – | – | – | – | – | – |
| 9 | [(Mo ₆ Br ₈)(OH) ₄ (H ₂ O) ₂] ^f | H ₂ | 400 | 23.5 | 0.0 | 19.0 | 0.0 | 0.0 | 18.8 | 6.6 | 32.5 | 20.0 |
| 10 | [(Ta ₆ Cl ₁₂)Cl ₂ (H ₂ O) ₄] · 4H ₂ O | H ₂ | 400 | 20.1 | 3.7 | 4.2 | 81.8 | 9.5 | 0.3 | 0.0 | 0.3 | 0.2 |
| 11 | (H ₃ O) ₂ [(W ₆ Cl ₈)Cl ₆] · 6H ₂ O | H ₂ | 400 | 11.7 | 7.9 | 76.2 | 0.3 | 0.0 | 0.7 | 1.1 | 6.6 | 7.2 |
| 12 | Re ₃ Cl ₉ | H ₂ | 400 | 3.7 | 4.9 | 4.6 | 1.7 | 0.0 | 1.3 | 2.0 | 42.9 | 42.6 |
| 13 | Mo metal | H ₂ | 400 | 0.0 | – | – | – | – | – | – | – | – |
| 14 | None | H ₂ | 400 | 0.0 | – | – | – | – | – | – | – | – |
| 15 | (H ₃ O) ₂ [(Mo ₆ Cl ₈)Cl ₆] · 6H ₂ O (1)/SiO ₂ ^g | H ₂ | 400 | 2.3 | 8.9 | 25.7 | 9.3 | 0.0 | 4.4 | 3.1 | 32.4 | 16.2 |
| 16 | MoO ₂ | H ₂ | 400 | 1.1 | 0.0 | 3.7 | 78.7 | 0.0 | 0.8 | 1.4 | 12.2 | 3.2 |

^a After treatment of cluster (200 mg) in a stream of carrier gas (300 mL/h) at 400 °C for 1 h, the reaction was initiated by introduction of *p*-diethylbenzene (0.40 mmol/h, 62 μL/h) into the carrier gas stream. Conversion = ((reacted material)/(reacted material + recovered material)) × 100 (%) 4 h after the reaction started. Selectivity = (product/(total amount of products)) × 100 (%) 4 h after the reaction started. No hydrogenolysis of the aromatic ring was observed 4 h after the reaction started. No disproportionation to triethylbenzenes was observed in all the reactions. Methane, ethane, and ethylene originating from the side chains are not taken into account.

^b H₂: 600 mL/h.

^c H₂: 1200 mL/h.

^d Pretreated at 400 °C in a stream of hydrogen for 1 h before reaction.

^e Pretreated at 300 °C in a stream of hydrogen for 1 h before reaction.

^f Naphthalene (3.1%).

^g 5.0 wt% of **1** was supported on silica gel (380 m²/g).

A halide cluster of tungsten, $(\text{H}_3\text{O})_2[(\text{W}_6\text{Cl}_8)\text{Cl}_6] \cdot 6\text{H}_2\text{O}$, a Group 6 metal, exhibited almost the same catalytic activity and selectivity with **1** (entry 11). On the other hand, a halide cluster of tantalum, $[(\text{Ta}_6\text{Cl}_{12})\text{Cl}_2(\text{H}_2\text{O})_4] \cdot 4\text{H}_2\text{O}$, a Group 5 metal, selectively catalyzed the dehydrogenation to yield *p*-ethylstyrene and a small quantity of *p*-divinylbenzene (entry 10). A cluster of niobium, $[(\text{Nb}_6\text{Cl}_{12})\text{Cl}_2(\text{H}_2\text{O})_4] \cdot 4\text{H}_2\text{O}$, also a Group 5 metal, showed intermediate selectivity with respect to the above clusters, forming both *m*-dimethylbenzene and *p*-ethylstyrene in significant quantities (entry 1). Trirhenium nonachloride, Re_3Cl_9 , is reported to change to metallic rhenium on treatment with hydrogen at 250–300 °C [35], which was confirmed by our XRD analysis. This reduced Re selectively catalyzed the dealkylation of the side chain (Eq. (2)) to yield ethylbenzene and dealkylation in the side chain (Eq. (5)) to yield *p*-ethyltoluene (entry 12). One of the main effects of platinum in bifunctional Pt/Al₂O₃–ZSM-5 catalyst in the transformation of ethylbenzene is to increase the rate of dealkylation [36]. A similar effect has been reported for Pt/Al₂O₃–zeolite catalysts in ethylbenzene hydroisomerization [37]. Rhenium is located in a neighboring position to the platinum group metals in the Periodic Table, and is similar to the platinum group metals in some of its properties. Rhenium metal, as well as its oxide, sulfide, and selenide, is a catalyst in the hydrogenation of organic compounds [38,39].

Compound **1** supported on silica gel was also an active catalyst. However, its selectivity differed (entry 15). The surface hydroxyl group of the silica gel is a likely participant in the catalysis reaction.

3.4. Application of **1** to disubstituted benzenes

Table 2 summarizes the catalytic activity of **1** for some *p*-substituted benzenes. All substrates tested, except *p*-cymene, yielded the corresponding *m*-isomer as the main product by ring-attachment isomerization. The halide cluster cata-

lysts, which have no micropores, are shown to be applicable to the isomerization of long-chain alkyl compounds. *p*-Cymene exhibited quite high reactivity, but the reaction pathway changed to dealkylation, yielding toluene, which can be ascribed to the formation of a stable secondary carbenium ion as an intermediate [22]. *p*-Propyltoluene yielded *p*-cymene in 6.0% selectivity by a skeletal rearrangement of the *n*-alkyl group to the secondary alkyl group, which indicates that a carbenium ion had formed in this case [20].

As Table 3 shows, three diethylbenzene isomers reacted over **1** to achieve similar conversions, with the main reaction being ring-attachment isomerization, although the selectivity for the isomerization decreased in the order *p*- > *m*- > *o*- isomer. Even traces of triethylbenzenes (Eq. (4)) were not detected in all the reactions. The selectivities for mutual interconversion of the three isomers are illustrated in Fig. 4. One of the most striking features of the reactions is that *o*-diethylbenzene afforded the *m*-isomer in a selectivity that was three times that of the *p*-isomer, even though from a thermodynamical point of view, the *p*-isomer is more stable than the *m*-isomer [40]. *p*-Diethylbenzene yielded predominantly its *m*-isomer, which was only twice as abundant as the equilibrium composition, compared with the *o*-isomer. On the other hand, the *m*-isomer afforded the sterically hindered *o*-isomer more abundantly than expected from the equilibrium composition, when compared with the formation of the *p*-isomer. Consequently, the ethyl group preferentially migrated to the neighboring position of the aromatic ring, irrespective of the equilibrium distribution.

When a mixture of *p*-xylene and *p*-diethylbenzene was applied to the reaction, ring-attachment isomerization occurred to yield the corresponding *o*- and *m*-isomers, as shown in Table 2. However, the formation of *o*- and *m*-ethyltoluenes, which would be expected from intermolecular alkyl transfer, was not detected. Furthermore, triethylbenzenes were not detected in any of the reactions listed in Tables 1–3. These results clearly demonstrate that the iso-

Table 2
Isomerization and dehydrogenation of *p*-disubstituted benzenes^a

| Substrate | Conversion (%) | Selectivity (%) | | | | | | | | |
|---|----------------|------------------|------------------|-----------------|--------------|---------|--------------|------------------|------------------------|------------------|
| | | Isomerization | | Dehydrogenation | Dealkylation | | | | | Others |
| | | <i>o</i> -Isomer | <i>m</i> -Isomer | | Benzene | Toluene | Ethylbenzene | <i>p</i> -Xylene | <i>p</i> -Ethyltoluene | |
| <i>p</i> -Xylene | 13.9 | 5.3 | 71.3 | – | 1.7 | 13.4 | – | – | – | 8.3 ^b |
| <i>p</i> -Ethyltoluene | 11.8 | 6.0 | 75.6 | 2.9 | 1.6 | 11.4 | 1.7 | 0.8 | – | 0.0 |
| <i>p</i> -Propyltoluene | 9.4 | 3.7 | 52.6 | 23.2 | 0.0 | 11.3 | 0.0 | 1.3 | 1.9 | 6.0 ^c |
| <i>p</i> -Cymene | 76.5 | 0.3 | 10.7 | 0.1 | 0.1 | 86.6 | 0.0 | 0.1 | 0.0 | 2.1 ^d |
| <i>p</i> -Diethylbenzene | 9.5 | 7.7 | 74.0 | 4.9 | 2.7 | 0.5 | 9.4 | 0.0 | 0.8 | 0.0 |
| $\left\{ \begin{array}{l} \textit{p}\text{-Xylene} \\ + \\ \textit{p}\text{-Diethylbenzene}^{\text{e}} \end{array} \right.$ | 5.6 | 1.0 | 5.6 | – | 6.3 | 11.1 | – | – | – | – |
| | | 8.7 | 50.6 | 0.0 | | | 5.2 | 0.7 | 10.8 ^f | |

^a Reactions were performed at 400 °C using 0.40 mmol/h substrate. The other conditions are the same as described for Table 1.

^b Ethylbenzene (1.2%), 1,2,3-trimethylbenzene (0.6%), 1,2,4-trimethylbenzene (6.3%), and 1,3,5-trimethylbenzene (0.2%).

^c *p*-Cymene.

^d *p*-Propyltoluene (1.8%) and *m*-propyltoluene (0.3%).

^e Mixture of *p*-xylene (0.20 mmol/h) and *p*-diethylbenzene (0.20 mmol/h). The selectivity is based on the total mass of starting materials.

^f *p*-Divinylbenzene (10.8%). *o*-Ethyltoluene and *m*-ethyltoluene were not detected.

Table 3
Reaction of diethylbenzenes and ethylbenzene over $(\text{H}_3\text{O})_2[(\text{Mo}_6\text{Cl}_8)\text{Cl}_6] \cdot 6\text{H}_2\text{O}$ (1)^a

| Substrate | Conversion (%) | Selectivity (%) | | | | | | | |
|---------------------------------------|----------------|------------------|------------------|------------------|-----------------|---------------------------|---------|--------------|------------------|
| | | Isomerization | | | Dehydrogenation | Dealkylation ^b | | | |
| | | <i>o</i> -Isomer | <i>m</i> -Isomer | <i>p</i> -Isomer | | Benzene | Toluene | Ethylbenzene | Ethyltoluene |
| <i>o</i> -Diethylbenzene | 6.3 | – | 31.7 | 10.9 | 26.2 | 2.2 | 1.4 | 27.5 | 0.1 |
| <i>m</i> -Diethylbenzene | 7.9 | 26.8 | – | 47.7 | 7.6 | 2.7 | 0.8 | 11.1 | 3.2 ^c |
| <i>p</i> -Diethylbenzene | 9.5 | 7.7 | 74.0 | – | 4.9 | 2.7 | 0.5 | 9.4 | 0.8 |
| <i>p</i> -Diethylbenzene ^d | 1.7 | 7.7 | 10.6 | – | 58.8 | 7.1 | 0.7 | 7.5 | 7.6 |
| Ethylbenzene | 0.3 | – | – | – | 61.5 | 26.7 | 11.8 | – | – |
| Ethylbenzene ^d | 2.9 | – | – | – | 88.0 | 8.1 | 3.9 | – | – |

^a Reactions were performed at 400 °C using 0.40 mmol/h substrate. The other conditions are the same as listed for Table 1. Disproportionation to yield triethylbenzenes from diethylbenzenes or diethylbenzenes from ethylbenzene was not detected in all the reactions.

^b *o*-, *m*-, and *p*-isomerism was retained unless otherwise noted. Xylenes were not detected.

^c *m*-Ethyltoluene (2.2%) and *p*-ethyltoluene (1.0%).

^d In He stream.

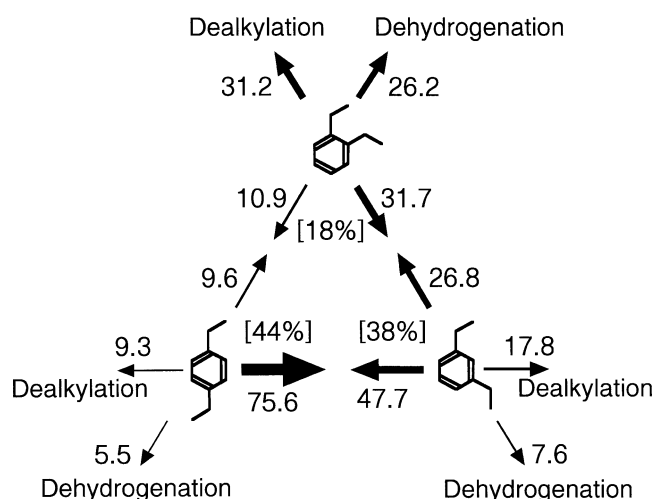


Fig. 4. Isomerization of diethylbenzenes over $(\text{H}_3\text{O})_2[(\text{Mo}_6\text{Cl}_8)\text{Cl}_6] \cdot 6\text{H}_2\text{O}$ (1), showing the selectivity values (in %) at 400 °C, 4 h after the reaction was initiated. No hydrogenolysis of the aromatic ring was observed. Methane, ethane, and ethylene originating from the side chain are not taken into account. The other reaction conditions are the same as those described in the caption to Fig. 1. The thickness of each arrow is proportional to the corresponding selectivity. The equilibrium compositions of diethylbenzenes in the vapor phase at 400 °C are shown in brackets.

merization proceeded via an intramolecular 1,2-shift of the alkyl group around the aromatic ring.

3.5. Development of active sites

XRD patterns of the pretreated samples at various temperatures in a hydrogen stream for 1 h are shown in Fig. 5, with that of the $\text{Mo}_6\text{Cl}_{12}[(\text{Mo}_6\text{Cl}_8^i)\text{Cl}_4^a(\text{H}_2\text{O})_2]$ (2) samples being synthesized independently. The sample heat-treated at 200 °C was assignable to $[(\text{Mo}_6\text{Cl}_8^i)\text{Cl}_4^a(\text{H}_2\text{O})_2]$ (3) [41,42]. Fig. 5 shows that cluster 1 changed above 100 °C from 1 via 3 to the extended Mo–Cl–Mo bonded solid-state cluster 2 as heat was applied up to 400 °C (Eqs. (6) and (7), Scheme 1). An increase of about 50% in the surface area was observed

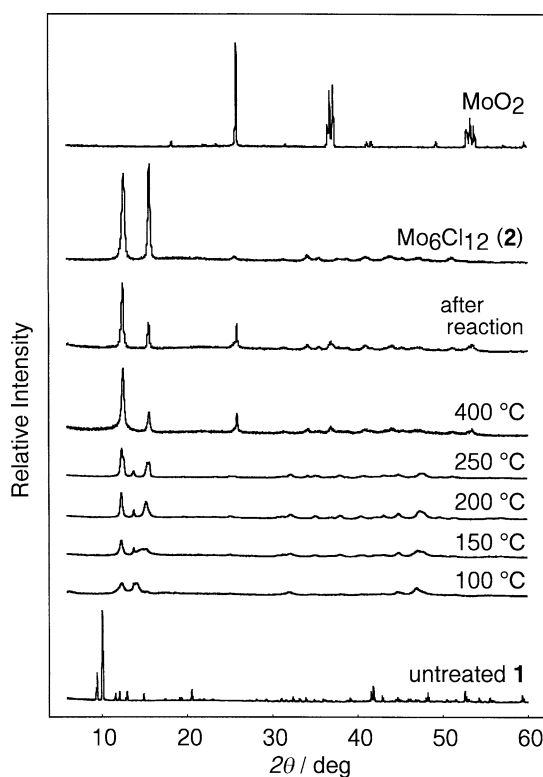
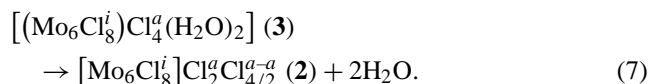
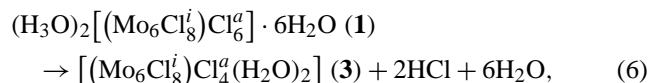
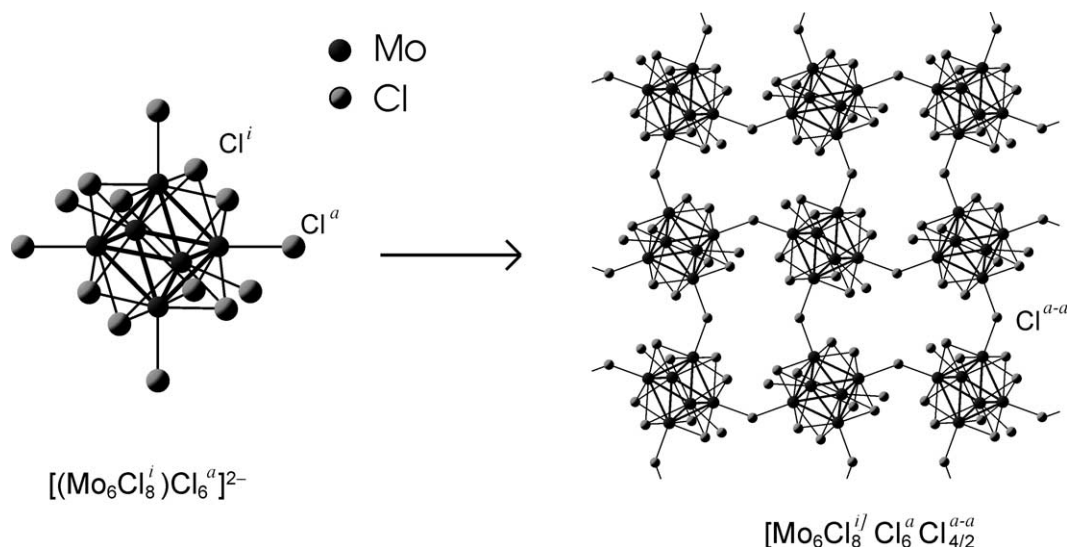


Fig. 5. XRD patterns of $(\text{H}_3\text{O})_2[(\text{Mo}_6\text{Cl}_8)\text{Cl}_6] \cdot 6\text{H}_2\text{O}$ (1) treated at various temperatures with H_2 (300 mL/h) for 1 h. The XRD patterns of 1 subjected to 4 h reaction at 400 °C, $\text{Mo}_6\text{Cl}_{12}$ (2), and MoO_2 are also shown.

after the pretreatment.



The same trends were observed in Raman spectroscopy. Raman spectra of the samples discussed above are shown in Fig. 6, in which four assigned peaks [43] are retained up to 200 °C. Above this temperature, the Raman peak orig-



Scheme 1.

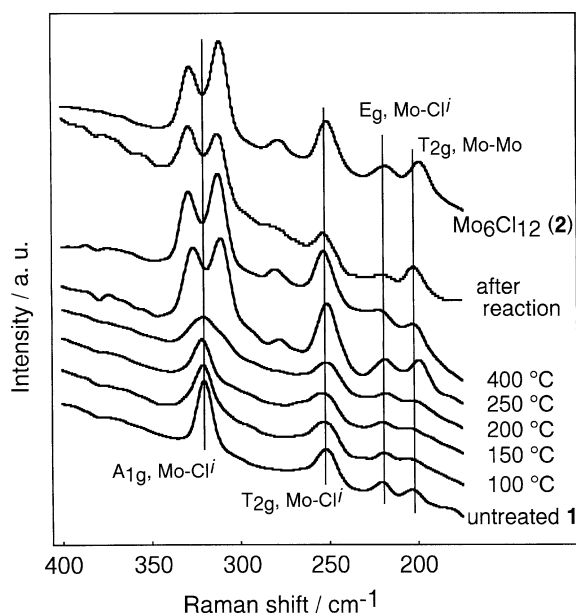


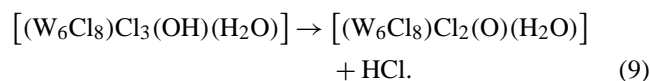
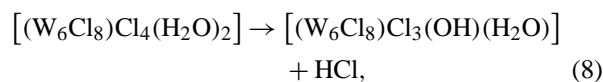
Fig. 6. Raman spectra of $(\text{H}_3\text{O})_2[(\text{Mo}_6\text{Cl}_8)\text{Cl}_6] \cdot 6\text{H}_2\text{O}$ (**1**) treated at various temperatures with H_2 (300 mL/h) for 1 h. The Raman spectra of **1** subjected to 4 h reaction at 400 °C and $\text{Mo}_6\text{Cl}_{12}$ (**2**) are also shown. No Raman peaks attributable to MoO_2 were observed in this region.

inally at 321 cm^{-1} ascribed to the triple bridged Mo-Clⁱ breathing vibration was replaced by two peaks, suggesting a change in the coordination mode, and a new peak appeared at 278 cm^{-1} . It is at this temperature that catalytic activity emerged. No appreciable change in the XRD patterns and the Raman spectra after a 5-h reaction time was observed with *p*-diethylbenzene at the same temperatures.

The Raman spectrum of **1** heat treated at 400 °C was almost the same as that of a sample of cluster **2**. However, closer examination of the XRD patterns shows that the crystallinity of **1** heat-treated was poor, and that it contained a small quantity of MoO_2 . This indicated that the

coordinated water had not been completely removed by pretreatment, and that the oxygen of the water molecules had been captured to form MoO_2 at 400 °C. The synthesis of **2** from **1** is performed by gradual heating up to 200 °C, followed by prolonged heating at the same temperature under vacuum. The coordinated water is removed by this heat treatment, and is replaced with bridging Cl^{a-a} ligands (Scheme 1). Rapid heating to higher temperatures would give rise to the formation of imperfect crystals containing defective $[\text{Mo}_6\text{Cl}_8^i]\text{Cl}_2^a\text{Cl}_{4/2}^{a-a}$ moieties, and exhibiting catalytic activity, as in the case of olefin isomerization on $(\text{H}_3\text{O})_2[(\text{W}_6\text{Cl}_8)\text{Cl}_6] \cdot 6\text{H}_2\text{O}$ [**1**].

We have reported on the catalytic isomerization of olefins, dehydration of alcohols, dehydrohalogenation of halogenated alkanes, and decomposition of phenyl acetate to phenol and ketene by halide cluster catalysts, as mentioned above. All of these reactions are catalyzed by conventional solid acids and bases, and the evolution of HCl was observed on pretreatment of the clusters. By taking into account the electronegativity of the metal, we deduced that the active sites on the cluster surface are hydroxo- (Eq. (8)) or oxo- (Eq. (9)) species as exemplified in the case of the W cluster. The ring-attachment isomerization would be catalyzed by this acidic species.



When a hydrogen gas stream was replaced with a helium gas stream in the reaction of *p*-diethylbenzene, the main reaction changed from isomerization to dehydrogenation (Table 3). In both cases, dealkylation proceeded significantly. Hydrogen favored isomerization, and was partly used for reductive dealkylations and, when in low concentration, it was taken from the substrate. Similarly, dehydrogenation of eth-

ylbenzene proceeded under a He stream, and, under both He and H₂ streams, dealkylation proceeded (Table 3). The latter reaction has not been reported for conventional molecular strong acids or for solid acid catalysts, except under cracking conditions. Dealkylation of ethylbenzene under hydrogen has been reported exclusively on platinum group metals and on Ni:Pt, Ni [44], and Rh [45] on SiO₂, Al₂O₃, or TiO₂ and Ni on mordenite [46]. Dealkylation of propylbenzene over Pt/SiO₂ or Al₂O₃ [47] and of pentylbenzene over Pt/silica–alumina catalysts [48] has been reported. Halide clusters of Group 6 metals always afforded dealkylation products in selectivities of 12–49% at 400 °C (Tables 1–3).

In the case of Group 6 metals, another type of active site can be envisaged. On heating of a more electronegative (Group 5 metal) Nb cluster containing aqua ligands, [(Nb₆Cl₁₂)Cl₂(H₂O)₄] · 4H₂O, the ligand is not lost, and hence a binary complex of [Nb₆Cl₁₄][Nb₆Cl₁₀Cl_{2/2}^{i-a}] Cl_{2/2}^{a-i} Cl_{4/2}^{a-a} is not formed, which can be synthesized by another route involving the comproportionation of Nb metal with NbCl₅ in a sealed Nb metal tube [49]. In contrast, the aqua ligands of **1** are easily removed by heating at 200 °C to yield the binary complex **2**, as mentioned above. Rhenium chloride, a Group 7 metal complex, is easily and completely reduced to metallic Re on heating in a hydrogen atmosphere at above 250 °C. Hence, coordinatively unsaturated or, more likely, hydrido ligands containing Mo or W metal could exist in the poorly crystallized samples of **2**.

In a series of Y(η⁵-C₅H₅)₂(alkyl), [Zr(η⁵-C₅H₅)₂(alkyl)]⁺, and [Nb(η⁵-C₅H₅)(η⁴-C₄H₆)]⁺ moieties, these metals are isoelectronic, exhibiting similar polymerization activities [50]. It is well known that Ru metals in RuCl₂(PPh₃)₃ and RuHCl(PPh₃)₃ are isoelectronic with Rh metal in RhCl(PPh₃)₃, and that these complexes are catalysts in the homogeneous hydrogenation of unsaturated C–C bonds [51]. Thus, Group 6 metal atoms of the halide cluster complexes could be isoelectronic with the platinum group metals by taking two or more electrons from the halogen and hydrido ligands. The selectivity for reductive dealkylation by the cluster complexes could be attributable to the metallic nature of the clusters.

4. Conclusions

The halide cluster (H₃O)₂[(Mo₆Cl₈)Cl₆] · 6H₂O (**1**) developed catalytic activity above 200 °C for *p*-diethylbenzene. The activity depended on reaction temperature, with dehydrogenation, ring-attachment isomerization, and dealkylation increasing with increasing temperature. Groups 5 and 6 metal halide clusters exhibited a characteristic selective ring-attachment isomerization of diethylbenzenes by the intramolecular 1,2-shift mechanism without yielding disproportionation products at 400 °C. They are distinct from conventional molecular strong acids, such as AlCl₃ and CF₃COOH, or solid acids, such as zeolite Y and ZSM-5, isomerization of which is based on an intermolecular transalky-

lation mechanism. Another characteristic feature of halide cluster catalysis is that the halide clusters have no micropore structures and, hence, they can be used to catalyze *o*-diethylbenzene, which is too large to enter the pores of zeolite Y and ZSM-5.

The isomerizations over cluster catalysts are always accompanied by an appreciable yield of dealkylation products under a hydrogen stream, particularly over Group 6 metal clusters. Dehydrogenation proceeds preferentially under a helium stream. Thus, atmospheric hydrogen, as well as alkyl hydrogen, is activated over these cluster catalysts, and can be used to carry out reductive dealkylations that have previously been reported over platinum group metal catalysts.

References

- [1] S. Kamiguchi, M. Noda, Y. Miyagishi, S. Nishida, M. Kodomari, T. Chihara, *J. Mol. Catal. A* 195 (2003) 159.
- [2] S. Kamiguchi, M. Watanabe, K. Kondo, M. Kodomari, T. Chihara, *J. Mol. Catal. A* 203 (2003) 153.
- [3] S. Kamiguchi, T. Chihara, *Catal. Lett.* 85 (2003) 97.
- [4] T. Chihara, S. Kamiguchi, *Chem. Lett.* (2002) 70.
- [5] L. Cejka, B. Wichterlova, *Catal. Rev. Sci. Eng.* 44 (2002) 375.
- [6] T.-C. Tsai, S.-B. Liu, I. Wang, *Appl. Catal. A* 181 (1999) 355.
- [7] W.W. Kaeding, G.C. Barile, M.M. Wu, *Catal. Rev. Sci. Eng.* 26 (1984) 597.
- [8] A.B. Halgeri, J. Das, *Catal. Today* 73 (2002) 65.
- [9] M.A.A. Kareem, S. Chand, I.M. Mishra, *J. Sci. Ind. Res.* 60 (2001) 319.
- [10] S. Zheng, A. Jentys, J.A. Lercher, *J. Catal.* 219 (2003) 310.
- [11] H. Manstein, K.P. Moller, W. Bohringer, C.T. O'Connor, *Micropor. Mesopor. Mater.* 51 (2002) 35.
- [12] S. Zheng, H. Heydenrych, P. Roeger, A. Jentys, J.A. Lercher, *Stud. Surf. Sci. Catal.* 135 (2001) 1772.
- [13] S.-H. Park, H.-K. Rhee, *Catal. Today* 63 (2000) 267.
- [14] J. Cejka, A. Krejci, *Stud. Surf. Sci. Catal.* 130C (2000) 2627.
- [15] A. Sassi, M.A. Wildman, H.J. Ahn, P. Prasad, J.B. Nicholas, J.F. Haw, *J. Phys. Chem. B* 106 (2002) 2294.
- [16] J.V. Cejka, A. Krejci, N.V. Zilkova, J.V. Dedecek, J.V. Hanika, *Micropor. Mesopor. Mater.* 44 (2001) 499.
- [17] E. Dumitriu, C. Guimon, V. Hulea, D. Lutic, I. Fechete, *Appl. Catal. A* 237 (2002) 211.
- [18] M. Brini, R. Mislin, J.-M. Sommer, *Bull. Soc. Chim. Fr.* (1965) 3654.
- [19] N. Nambu, K. Yamamoto, S. Hamanaka, M. Ogawa, *Nippon Kagaku Kaishi* (1979) 925.
- [20] H.J. Bakoss, R.M.G. Roberts, A.R. Sadri, *J. Org. Chem.* 47 (1982) 4053.
- [21] G.A. Olah, M.W. Meyer, N.A. Overchuk, *J. Org. Chem.* 29 (1964) 2313.
- [22] A.P. Bolton, M.A. Lanewala, P.E. Pickert, *J. Org. Chem.* 33 (1968) 1513.
- [23] R.H. Allen, L.D. Yats, D.S. Erley, *J. Am. Chem. Soc.* 82 (1960) 4853.
- [24] R.H. Allen, *J. Am. Chem. Soc.* 82 (1960) 4856.
- [25] J. Engelhard, *J. Catal.* 145 (1994) 574.
- [26] N. Arsenova-Härtel, H. Bludau, R. Schumacher, W.O. Haag, H.G. Karge, E. Brunner, U. Wild, *J. Catal.* 191 (2000) 326.
- [27] T. Yashima, J.-H. Kim, H. Ohta, S. Namba, T. Komatsu, *Stud. Surf. Sci. Catal.* 90 (1994) 379.
- [28] J.S. Beck, W.O. Haag, in: G. Ertl, H. Knözinger, J. Weitkamp (Eds.), *Handbook of Heterogeneous Catalysis*, vol. 5, Wiley-VCH, Weinheim, 1997, p. 2136.
- [29] F.W. Koknat, J.A. Parsons, A. Vongvusharintra, *Inorg. Chem.* 13 (1974) 1699.

- [30] P. Nannelli, B.P. Block, *Inorg. Synth.* 12 (1970) 170.
- [31] J.C. Sheldon, *J. Chem. Soc.* (1962) 410.
- [32] V. Kolesnichenko, L. Messerle, *Inorg. Chem.* 37 (1998) 3660.
- [33] L. Forni, S. Carra, *J. Catal.* 26 (1972) 153.
- [34] H.G. Karge, J. Ladebeck, Z. Sarbak, K. Hatada, *Zeolites* 2 (1982) 94.
- [35] H. Gehrke Jr., D. Bue, *Inorg. Synth.* 12 (1970) 193.
- [36] J.M. Silva, M.F. Ribeiro, F.R. Ribeiro, E. Benazzi, M. Guisnet, *Appl. Catal. A* 125 (1995) 1.
- [37] L.D. Fernandes, J.L.F. Monteiro, E.F. Sousa-Aguiar, A. Martinez, A. Corma, *J. Catal.* 177 (1998) 363.
- [38] W.H. Davenport, V. Kollonitsch, C.H. Kline, *Ind. Eng. Chem.* 60 (11) (1968) 10.
- [39] H.S. Broadbent, G.C. Campbell, W.J. Bartley, J.H. Johnson, *J. Org. Chem.* 24 (1959) 1847.
- [40] C.L. Yaws, P.Y. Chiang, *Chem. Eng.* 95 (1988) 81.
- [41] H. Schäfer, H. Plautz, H. Bauman, W. Beckmann, C. Brendel, U. Lange, H.-G. Schulz, R. Siepmann, *Z. Anorg. Allg. Chem.* 389 (1972) 57.
- [42] L.J. Guggenberger, A.W. Sleight, *Inorg. Chem.* 8 (1969) 2041.
- [43] J.R. Schoonover, T.C. Zietlow, D.L. Clark, J.A. Heppert, M.H. Chisholm, H.B. Gray, A.P. Sattelberger, W.H. Woodruff, *Inorg. Chem.* 35 (1996) 6606.
- [44] D. Duprez, A. Miloudi, G. Delahay, R. Maurel, *J. Catal.* 101 (1986) 56.
- [45] D. Duprez, A. Miloudi, G. Delahay, R. Maurel, *J. Catal.* 90 (1984) 292.
- [46] S. Narayanan, *J. Chem. Soc., Faraday Trans. 1* 75 (1979) 434.
- [47] S. Toppi, C. Thomas, C. Sayag, D. Brodzki, F.L. Peltier, C. Travers, G. Djéga-Mariadassou, *J. Catal.* 210 (2002) 431.
- [48] S.M. Csicsery, *J. Catal.* 15 (1969) 111.
- [49] A. Simon, H.G. Schnering, H. Wöhrle, H. Schäfer, *Z. Anorg. Allg. Chem.* 339 (1965) 155.
- [50] K. Mashima, *Macromol. Symp.* 159 (2000) 69.
- [51] M.A. Bennett, T.W. Matheson, in: G. Wilkinson, F.G.A. Stone, E.W. Abel (Eds.), *Comprehensive Organometallic Chemistry*, vol. 4, Pergamon Press, Oxford, 1982, p. 931.